Institut de Physique de l'Université de Neuchâtel

Réseaux de jonctions Josephson: effets de frustration et dynamique des vortex.

Thèse présentée à la Faculté des Sciences
de l'Université de Neuchâtel
pour l'obtention du grade de docteur ès sciences

par

Ricardo Théron
Physicien diplômé de l'Université de Neuchâtel

Mai 1992

IMPRIMATUR POUR LA THÈSE

Réseaux de jonctions Josephson: Effets de frustration et dynamique des vortex

de Monsieur Ricardo Théron

UNIVERSITÉ DE NEUCHÂTEL

FACULTÉ DES SCIENCES

La Faculté des sciences de l'Université de Neuchâtel
sur le rapport des membres du jury,

Messieurs P. Martinoli, H. Beck et B. Pannetier (Grenoble)

autorise l'impression de la présente thèse.

Neuchâtel, le 22 juin 1994

Le doyen:

H.-H. Nägeli

Observation of Domain-Wall Superlattice States in a Frustrated Triangular Array of Josephson Junctions

R. Théron,[1] S. E. Korshunov,[2] J. B. Simond,[1] Ch. Leemann,[1] and P. Martinoli[1]
[1]*Institut de Physique, Université de Neuchâtel, CH-2000 Neuchâtel, Switzerland*
[2]*L. D. Landau Institute for Theoretical Physics, Kosygina 2, 117334 Moscow, Russia*
(Received 25 August 1993)

A family of ground states at frustrations $f = \frac{1}{2} - \frac{1}{2}N^{-1}$, with N an integer ≥ 2, has been observed in the superfluid response of a triangular Josephson junction array as a function of the magnetic flux ($\propto f$) threading a unit cell. These states can be constructed by introducing one- or two-dimensional superlattices of domain walls on the background of the checkerboard ground state at $f = \frac{1}{2}$, the 1D superlattice (striped phase) being energetically more favorable for $N > 3$. A structural change of the ground state from the striped phase to a 2D superlattice of vacancies is predicted at $f_c \approx 0.468$.

PACS numbers: 74.50.+r, 75.10.Hk

The concept of frustration, first introduced by Toulouse [1], plays a fundamental role in modern condensed-matter physics and statistical mechanics. It is central, for instance, in the theoretical understanding of spin glasses, quasicrystals, and incommensurate systems. In this context, planar arrays of Josephson junctions exposed to a perpendicular magnetic field provide a unique system where the influence of a tunable level of frustration can be studied in a variety of topologies ranging from periodic to random structures, including quasiperiodic and fractal lattices. Such systems are a physical realization of the frustrated classical XY model where the degree of frustration is governed by a parameter f expressing the magnetic flux threading an elementary cell of the array in units of the superconducting flux quantum.

The determination of the ground state of a Josephson junction (JJ) array at arbitrary frustration is a delicate problem which has been addressed by several authors. In their pioneering work, Teitel and Jayaprakash [2], considering only rational f ($f = p/q$, p and q coprime integers) and assuming that the corresponding commensurate ground states of the vortex lattice are periodic with a $(q \times q)$ unit cell, were the first to determine the structure of a few low-order (small q) vortex configurations in a square JJ array. Relying on the same assumption, Halsey [3] subsequently conjectured that, for a selected class of frustrations (f rational and quadratic irrational) in the range $\frac{1}{3} \leq f \leq \frac{1}{2}$, the ground state of a square array has a quasi-one-dimensional "staircase" structure resulting in a "striped" phase characterized by a sequence of parallel *domain walls* separating $f = \frac{1}{2}$ "checkerboard" regions of opposite chirality. More recently, however, numerical calculations [4] revealed that, at large q, ground states close to $f = \frac{1}{2}$ no longer exhibit the $(q \times q)$ periodicity, thereby disproving, in part, Halsey's conjecture.

In this Letter, we focus on frustrated *triangular* JJ arrays and report the discovery of a new set of commensurate states which unambiguously demonstrates the central role of domain walls in determining the system's ground-state configurations. Besides their intrinsic relevance for the understanding of frustration, vortex dynamics, and critical phenomena in JJ arrays, our results should further stimulate the growing interest in studies probing the microscopic structure of magnetic vortex phases using novel imaging techniques [5].

Compared to other lattice structures, the potential-energy barrier opposing vortex motion in triangular JJ arrays is so low [6] that their superfluid (or diamagnetic) response $S(f)$ to a small low-frequency electromagnetic excitation is extremely sensitive to the fine tuning of f near a commensurate state. This distinctive feature results in an exceptionally rich fine structure [7] providing a unique laboratory to identify specific families of ground states. In the following we report measurements of $S(f)$ in which a particular sequence of quantum structures corresponding to commensurate states defined by $f = \frac{1}{2} - \frac{1}{2}N^{-1}$, where N is an integer such that $N \geq 2$, was observed. By a suitable choice of temperature, we were able to resolve structures up to $N = 8$. Relying on the observation that these structures appear at frustrations such that their deviation $\Delta f \equiv \frac{1}{2} - f = \frac{1}{2}N^{-1}$ from $f = \frac{1}{2}$ is *linear* in N^{-1}, we show that the corresponding states can be deduced from the checkerboard state at full frustration ($f = \frac{1}{2}$) by introducing *linear* defects creating either a one-dimensional (1D) superlattice of parallel domain walls (striped phase) or a two-dimensional (2D) periodic network of intersecting domain walls (hexagonal phase) separating $f = \frac{1}{2}$ regions of opposite chirality. Theoretical considerations reveal that the striped phase has the lowest energy for $N > 3$. Moreover, by comparing the energy of the striped phase to that of a competing 2D triangular superlattice of *pointlike* defects (vacancies) commensurate with the triangular vortex lattice at $f = \frac{1}{2}$, we find that the 2D vacancy superlattice becomes energetically more favorable for $f > f_c \approx 0.468$. However, being beyond experimental resolution, the structural crossover from the striped-phase to the vacancy-superlattice states was not observed.

The JJ array studied in this work is the same of the investigations of Ref. [7]. It consists of $\sim 10^6$ proximity-

0031-9007/94/72(4)/562(4)$06.00

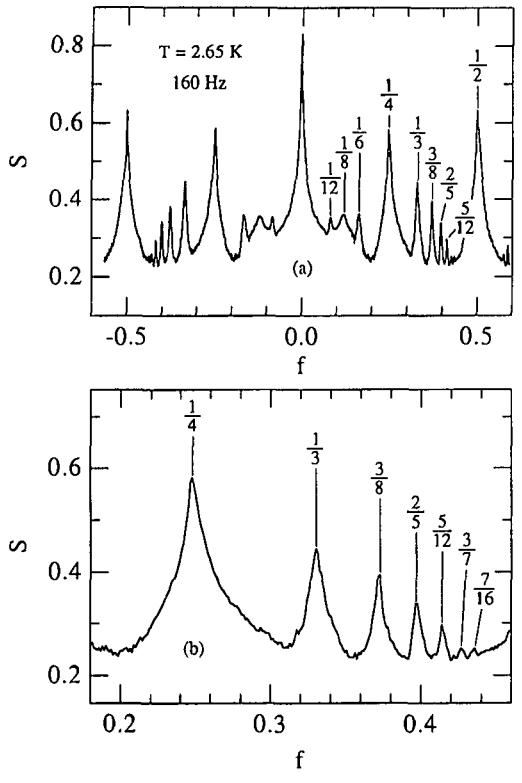

FIG. 1. (a) Normalized superfluid response of a triangular Josephson junction array as a function of frustration at 160 Hz; (b) expanded view of the interval $\frac{1}{4} < f < \frac{1}{2}$.

effect coupled Pb/Cu/Pb junctions sitting midway on the sides of a triangular lattice with a lattice spacing a of 15 μm. The superfluid response $S(f)$ was measured at 160 Hz with a SQUID-operated ac bridge detecting the mutual inductance change of a drive-receive coil system [8] induced by the supercurrents flowing in the JJ array in response to a weak ac field ($\sim$1 nT rms at the center of the array).

In Fig. 1 the superfluid response (normalized to that of a perfectly diamagnetic sample) is shown as a function of frustration at $T=2.65$ K or, more significantly, at $\tau=0.09$, where τ is the reduced temperature [6] relevant for the statistical mechanics of the system. At this temperature, superconducting phase coherence is expected to survive in a large number of commensurate states [9], but vortex-lattice defects created in their neighborhood by excess or missing vortices are still mobile enough [7] to sharpen the fine structure substantially, thereby enhancing resolution. Besides the central prominent peak at $f=0$ and weaker structures at $f=1/q$ with $q=6$, 8, and 12, $S(f)$ exhibits a characteristic sequence of sharp peaks at $f=\frac{1}{4}, \frac{1}{3}, \frac{3}{8}, \frac{2}{5}, \frac{5}{12}$ whose strength decreases with increasing q [Fig. 1(a)]. Expansion of the interval $\frac{1}{4} < f < \frac{1}{2}$ [Fig. 1(b)] reveals two additional peaks of the same series at $f=\frac{3}{7}$ and $f=\frac{7}{16}$. As shown in Fig. 2, the positions of these commensurate structures are very accurately fitted by the expression $f=\frac{1}{2}-\frac{1}{2}N^{-1}$ with $N=2,3,\ldots,7,8,\ldots$ showing that the sequence obeys the relation $\Delta f=\frac{1}{2}N^{-1}$.

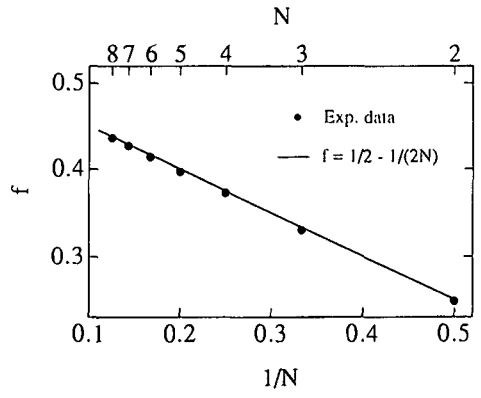

FIG. 2. Dependence of the peak positions of Fig. 1(b) on the inverse sequential integer N^{-1} and comparison with the relation $f=\frac{1}{2}-1/2N$.

In order to elucidate the nature of the commensurate states at $f=\frac{1}{2}-\frac{1}{2}N^{-1}$, we first recall that the ground state at $f=\frac{1}{2}$ has a checkerboardlike structure consisting of elementary triangular cells with alternating positive and negative vorticities. In a Coulomb gas representation [3,10], such a state can be conceived of as a lattice of negative (positive) integer vortex charges on a positive (negative) background. To ensure global charge neutrality, for $f<\frac{1}{2}$ charged defects must appear on the background of the regular checkerboard state in order to make the actual vortex density less than that at $f=\frac{1}{2}$. Since the structure of the ground state at $f=\frac{1}{2}$ allows for the creation of both pointlike (vacancies) and linear (domain walls) defects, there are three main possibilities to construct ground states in the vicinity of $f=\frac{1}{2}$: (i) a 2D lattice of vacancies, (ii) a 1D sequence of parallel domain walls, and (iii) a 2D network of crossing (or possibly ramifying) domain walls of different orientations. Also, the possibility of ground states in which both pointlike and linear defects are present [11] cannot be excluded *a priori*.

A ground state involving some regular arrangement of defects is expected to be more stable against thermal fluctuations when it is *commensurate* with the underlying lattice. This occurs if $\mathbf{g}=\mathbf{q}$, where g is a vector of the reciprocal defect lattice and $\mathbf{q}$ a wave vector describing the modulation provided by the (triangular) substrate. In particular, an equilateral triangular superlattice of vacancies is commensurate with the triangular lattice of vortices in the $f=\frac{1}{2}$ ground state [Fig. 3(c)] if $\Delta f=[2(L^2+M^2-LM)]^{-1}$, where L and M are integers. For all other (intermediate) values of f the periodic 2D force field created by the underlying lattice will deform the "natural" triangular superlattice of vacancies, thereby making it more vulnerable to thermal fluctuations.

Within the family of vacancy-superlattice states, the most symmetric ones, corresponding to orientations such that $L=M$ and $L=-M$, are expected to be the most

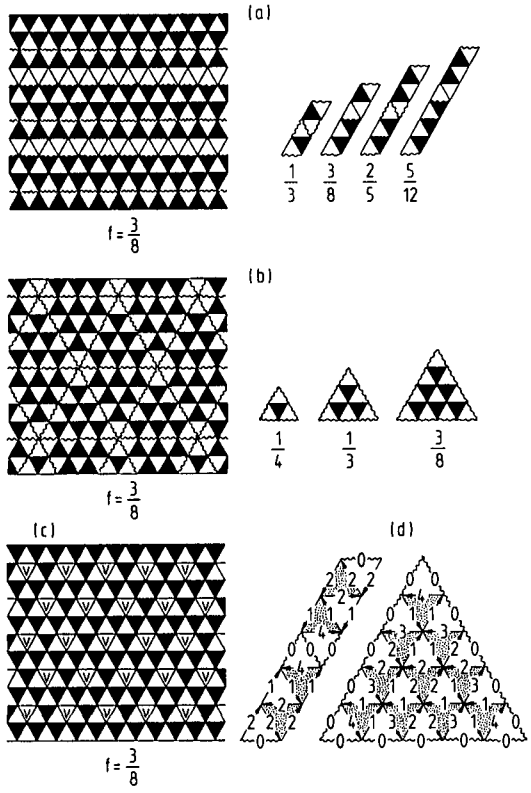

FIG. 3. Structure of (a) the striped phase, (b) the hexagonal phase, and (c) the vacancy (V) superlattice phase for $f=\frac{3}{8}$. In (a) and (b) a few superlattice elementary cells at other $f=\frac{1}{2}-1/2N$ are also shown. Wavy lines denote domain walls. (d) Distribution of the gauge-invariant phase differences (in units of $\pi/5$) at $f=\frac{2}{5}$ in the elementary cells of the striped and hexagonal phases.

stable ones. Structures in $S(f)$ arising from such states should therefore occur at frustrations such that $\Delta f \propto M^{-2}$, in striking contrast with the linear dependence of Δf on N^{-1} emerging from the data of Fig. 2. This strongly supports the idea that the sequence of peaks observed in $S(f)$ corresponds to a set of ground states which stem from the $f=\frac{1}{2}$ state by introducing a system of linear defects (domain walls) commensurate with the underlying lattice.

We have constructed two sets of states, one based on a 1D sequence of parallel domain walls [striped phase, Fig. 3(a)] and the other on a 2D triangular network of intersecting domain walls [hexagonal phase, Fig. 3(b)], and discovered that both families correspond to the series of peaks at $f=\frac{1}{2}-\frac{1}{2}N^{-1}$ observed in $S(f)$. As it is impossible to discriminate between the two configurations on the basis of the experimental data, it is necessary to compare their energies. By imposing supercurrent conservation at the nodes and fluxoid quantization in the triangular loops of the array, the distribution of the gauge-invariant phase differences $\{\theta_{ij}\}$ on the bonds $\langle ij\rangle$ of the lattice can be found explicitly for both families of states. As shown in Fig. 3(d) for $f=\frac{2}{5}$, this results in a very regular pattern exhibiting simple recursive properties. Summation of the bond contributions $\{-J\cos\theta_{ij}\}$, where J is the Josephson coupling energy, shows (see Table I) that the energy (per site) E_S of the striped phase

$$E_S=-\frac{J}{N}\sum_{m=0}^{N-1}\left[2\cos\frac{\pi(N-1-2m)}{2N}+\cos\frac{2\pi m}{N}\right]=-\frac{2J}{N\sin\pi/2N} \quad (1)$$

is always lower, if $N>3$, than the energy E_H of the hexagonal phase:

$$E_H=-\frac{3J}{N^2}\sum_{m=1-N}^{N-1}(N-|m|)\cos\frac{\pi m}{N}=-\frac{6J}{N^2(1-\cos\pi/N)}. \quad (2)$$

For $N=3$ ($f=\frac{1}{3}$) Eqs. (1) and (2) predict $E_S=E_H=-4J/3$. However, as shown by free-energy calculations [12], at nonzero temperatures spin-wave-like excitations of the phase system remove the degeneracy favoring the hexagonal phase for a strictly sinusoidal current-phase relation. Similar considerations show that, among the various regular domain-wall structures [10] which correspond to the ground state at $f=\frac{1}{4}$ ($N=2$), the hexagonal phase is the most stable against thermal fluctuations [12].

It is important to notice that in the limit $N\to\infty$ ($f\to\frac{1}{2}$) both E_S and E_H are larger than $E_0=-3J/2$, the energy of the ground state at $f=\frac{1}{2}$ [9], implying that the energy of the linear defects does not vanish at arbitrarily small defect concentrations, i.e., for $\Delta f\to 0$. This is a manifestation of the long-range Coulomb interaction between pointlike defects in two dimensions and of the fact that linear defects can be

TABLE I. Comparison of the energies (per site and in units of J) of the striped phase (E_S), the hexagonal phase (E_H), and the vacancy-superlattice phase (E_V) at frustration $f=\frac{1}{2}-\frac{1}{2}N^{-1}$.

N	E_S	E_H	E_V
2		−1.5000	
3	−1.3333	−1.3333	−1.1133
4	−1.3066	−1.2803	−1.0607
5	−1.2944	−1.2567	
6	−1.2879	−1.2440	
7	−1.2840	−1.2365	−1.1453
8	−1.2815	−1.2316	
9	−1.2797	−1.2283	−1.1869
...			
12	−1.2769	−1.2228	−1.2341
...			
16	−1.2753	−1.2198	−1.2783
...			
∞	−1.2732	−1.2159	−1.5000

thought of as a superposition of pointlike defects [11]. By adding up the logarithmic potentials of pointlike defects to a "Coulomb potential" of a linear defect varying as $|x|$ in the direction x perpendicular to the wall and taking into account the compensating screening effect provided by the background, the total energy density of an infinite sequence of equally charged domain walls turns out to be finite and independent of the wall concentration.

On the other hand, calculations of the energy E_V of the vacancy superlattice show that E_V should approach E_0 with decreasing vacancy concentration. Thus, for frustrations sufficiently close to $f=\frac{1}{2}$ the true ground state should have the structure of a vacancy superlattice [Fig. 3(c)]. Unlike E_S and E_H, however, no general analytic expression can be derived for E_V, which was computed from the $\{\theta_{ij}\}$ of a few vacancy-superlattice states satisfying both $\Delta f=[2(L^2+M^2-LM)]^{-1}$ and $\Delta f=\frac{1}{2}N^{-1}$. As shown in Table I, where E_S, E_H, and E_V are compared, the striped phase has the lowest energy in the interval $\frac{1}{3}<f<f_c$ with $f_c\approx 0.468$, whereas for $f_c<f<\frac{1}{2}$ the vacancy superlattice is the most favorable configuration. Notice that, in this respect, the situation is similar to that found for square JJ arrays where, however, $f_c\approx 0.438$ [4]. Since structures corresponding to commensurate states near f_c are too weak to be resolved in our $S(f)$ measurements, the crossover from the striped-phase sequence ($\Delta f\propto N^{-1}$) to the vacancy-superlattice series ($\Delta f\propto M^{-2}$) was not observed.

Before concluding, we would like to stress that the calculations of E_S, E_H, and E_V were performed for an array with infinite penetration depth $\lambda_\perp$ [6]. For finite $\lambda_\perp$, cell self-inductance and mutual inductance coupling between cells [13] will affect the energy calculations. However, since $\lambda_\perp/a\approx 30$ at the temperature of interest ($T=2.65$ K), corrections are expected to be small and the overall picture emerging from our study will not be significantly modified. This conclusion is corroborated by the observation that the sequence at $f=\frac{1}{2}-\frac{1}{2}N^{-1}$, although less rich ($N<8$), persists at higher temperatures where $\lambda_\perp$ becomes comparable to the sample size and finite-$\lambda_\perp$ corrections are irrelevant.

In conclusion, high-resolution measurements of the superfluid response of a triangular Josephson junction array exposed to a magnetic field have provided novel insight into the nature of the ground state of a frustrated system. We have shown that a particular family of commensurate states observed at frustrations f such that $f=\frac{1}{2}-\frac{1}{2}N^{-1}$, where N is an integer ≥ 2, can be constructed from the checkerboard state at $f=\frac{1}{2}$ by introducing either a one-dimensional superlattice of parallel domain walls (striped phase) or a two-dimensional triangular superlattice of intersecting domain walls (hexagonal phase). The striped phase was found to have the lowest energy for $N>3$. Although not observed in our experiment, the ground state is predicted to undergo a structural transition from the striped phase to a two-dimensional superlattice of vacancies at a critical frustration $f_c\approx 0.468$.

One of us (P.M.) would like to thank S. Teitel for a clarifying discussion on domain walls. This work was supported by the Swiss National Science Foundation.

[1] G. Toulouse, Commun. Phys. **2**, 115 (1977).
[2] S. Teitel and C. Jayaprakash, Phys. Rev. Lett. **51**, 1999 (1983).
[3] T. C. Halsey, Phys. Rev. B **31**, 5728 (1985); Physica (Amsterdam) **152B**, 22 (1988).
[4] M. R. Kolahchi and J. P. Straley, Phys. Rev. B **43**, 7651 (1991); J. P. Straley and G. M. Barnett, Phys. Rev. B **48**, 3309 (1993).
[5] H. D. Hallen *et al.*, Phys. Rev. Lett. **71**, 3007 (1993); L. N. Vu *et al.*, Appl. Phys. Lett. **63**, 1693 (1993).
[6] C. J. Lobb *et al.*, Phys. Rev. B **27**, 150 (1983).
[7] R. Théron *et al.*, Phys. Rev. Lett. **71**, 1246 (1993).
[8] B. Jeanneret *et al.*, Appl. Phys. Lett. **55**, 2336 (1989).
[9] W. Y. Shih and D. Stroud, Phys. Rev. B **30**, 6774 (1984).
[10] S. E. Korshunov, J. Stat. Phys. **43**, 17 (1986).
[11] S. Teitel, Physica (Amsterdam) **152B**, 30 (1988).
[12] A. Vallat, S. E. Korshunov, and H. Beck (private communication).
[13] J. R. Phillips *et al.*, Phys. Rev. B **47**, 5219 (1993).

Evidence for Nonconventional Vortex Dynamics in an Ideal Two-Dimensional Superconductor

R. Théron, J.-B. Simond, Ch. Leemann, H. Beck, and P. Martinoli
Institut de Physique, Université de Neuchâtel, CH-2000 Neuchâtel, Switzerland

P. Minnhagen
Department of Theoretical Physics, Umeå University, S-90187 Umeå, Sweden
(Received 7 April 1993)

Impedance measurements performed on a weakly frustrated triangular array of Josephson junctions over a wide range of frequencies and at temperatures such that vortex pinning is irrelevant reveal that vortex dynamics in an ideal two-dimensional (2D) superconductor does not obey Drude's classical prediction for a 2D Coulomb gas of free and independent vortex charges. An analysis in terms of a complex vortex dielectric constant implies that the vortex mobility vanishes logarithmically in the limit of small frequencies, thereby pointing to anomalous vortex diffusion.

PACS numbers: 74.60.Ge, 74.25.Nf, 74.50.+r

The concept of vortex is essential to understand the physics of two-dimensional (2D) superfluids [1]. In neutral superfluids and, under appropriate conditions, in charged superfluids the interaction between two vortices depends logarithmically on their separation, a feature leading to a natural description of the vortex medium in terms of a 2D Coulomb gas analog [2]. Detailed insight into the physics of 2D superfluids emerging from this picture is provided by studies of their response to a time-dependent perturbation. The Andronikashvili torsional oscillator has proven to be quite successful to investigate vortex dynamics near the Kosterlitz-Thouless (KT) transition of liquid-helium films [3]. A corresponding probe for 2D superconductors relies on a two-coil mutual inductance technique [4] which allows us to extract the dynamical properties of the vortices from measurements of the sample's complex sheet impedance [5,6]. However, the experiments performed so far on liquid-helium films could not systematically explore the response as a function of frequency, while the investigations carried out on superconducting films [7] were almost unvariably affected by pinning effects masking the intrinsic 2D Coulomb-gas properties of the vortex medium. In this Letter, we report a study of the complex dielectric constant $\varepsilon(\omega)$ of a dilute system of vortices created by a small perpendicular magnetic field H in an almost pinning-free triangular array of Josephson junctions. Our data, taken over a wide range of driving angular frequencies ω, reveal novel and unexpected aspects of the dynamics of vortex excitations in an ideal, i.e., pinning-free, 2D superconductor.

Compared to superconducting films, Josephson junction arrays (JJA) prepared with modern microfabrication techniques provide nearly ideal systems in which vortex pinning due to ever present disorder can be kept at extremely low levels. Moreover, in *triangular* arrays intrinsic pinning effects resulting from the periodic nature of the system are much weaker than in other lattice structures and become totally irrelevant at temperatures T appreciably lower than the zero-field KT transition temperature T_{KT} [8]. Thus, if T is not too far below T_{KT} and H corresponds to small values (<0.05) of the frustration parameter f, defined as the number of flux quanta per elementary triangular cell, one would expect the vortex medium in a triangular JJA to behave as a 2D Coulomb gas of free (i.e., unpinned) and independent (i.e., noninteracting) charges with $\varepsilon(\omega)$ obeying Drude's classical prediction [9]. Surprisingly, however, we find that $\varepsilon(\omega)$, as inferred from measurements of the linear complex sheet impedance $Z=R+i\omega L$ of the array, is highly nonconventional at low frequencies. More precisely, the low-frequency superfluid component, $\mathrm{Re}[1/\varepsilon(\omega)]$, of $1/\varepsilon(\omega)$ is found to be proportional to ω, in striking contrast with the quadratic frequency dependence predicted by Drude's theory. This unusual dynamic response implies that the vortex mobility $\mu_v(\omega)$ vanishes as $1/|\ln\omega|$ in the limit $\omega\rightarrow 0$, a feature pointing to anomalously slow ("sluggish") vortex diffusion.

Although our results, in particular the logarithmic frequency dependence of $\mu_v(\omega)$, suggest a few attractive, though speculative, theoretical interpretations, the exact nature of the microscopic mechanism responsible for anomalous vortex transport has not been identified yet. We notice, however, that features identical to those observed in our measurements have been seen [10] in numerical simulations, based on a time-dependent Ginzburg-Landau approach, of the dynamic response of thermally nucleated free vortices in unfrustrated ($f=0$) square arrays. This supports the idea that anomalous vortex diffusion is a general *intrinsic* property of ideal 2D superfluids.

The JJA studied in this work is a system of $\sim 10^6$ *SNS* junctions consisting of star-shaped superconducting (S) Pb islands at the sites of a triangular lattice with lattice spacing $a=15$ μm and proximity effect coupled to each other by an underlying Cu normal (N) layer. In zero magnetic field the array undergoes a KT transition at $T_{KT}\approx 3.70$ K. Real and imaginary parts of Z were extracted [4] from measurements of the mutual inductance change of a drive-receive coil system induced by the supercurrents flowing in the JJA in response to a weak ac

0031-9007/93/71(8)/1246(4)$06.00

field creating a maximum rms flux smaller than $10^{-4}\phi_0$ per unit cell in the center of the array (ϕ_0 is the superconducting flux quantum). Combined with a suppression of ambient magnetic fields to ~ 1 mG, this low-level excitation allowed f to be tuned with a precision better than 10^{-3}. Data were taken over three decades in frequency, from 10 Hz to 10 kHz, with a SQUID-operated ac bridge allowing one to detect inductance changes of the order of 0.1 pH over most of the spectral range. In the following, temperatures will be expressed in terms of the reduced temperature $\tau = kT/E_J(T)$, where the Josephson coupling energy $E_J(T) = (\phi_0/2\pi)^2/[L_k(T)\sqrt{3}]$ was inferred from measurements of the "bare" sheet kinetic inductance $L_k(T)$ of the unfrustrated ($f=0$) array at temperatures well below T_{KT} [6].

In Fig. 1 the inverse inductive component L^{-1}, proportional to the effective (i.e., renormalized by various kinds of topological excitations) areal superfluid density in the system, is shown as a function of f at $\tau = 0.09$ ($T = 2.65$ K). The extraordinary richness of the fine structure with sharp peaks corresponding to commensurate states at $f = 0, \frac{1}{12}, \frac{1}{8}, \frac{1}{6}, \frac{1}{4}, \frac{1}{3}, \frac{3}{8}, \frac{2}{5}, \frac{5}{12}$, and $\frac{1}{2}$ and incipient higher-order maxima at $\frac{3}{7}$ and $\frac{7}{16}$ is a striking demonstration of the excellent uniformity of the array. With increasing temperature and/or decreasing frequency the fine structure in $L^{-1}(f)$ sharpens quite dramatically into a sequence of δ-function-like peaks [11]. We interpret this behavior as clear evidence that, at sufficiently high temperatures, phase coherence in the neighborhood of a commensurate state (where the vortex lattice is pinned) is drastically disrupted by excess (or missing) vortices moving *freely* on a pinned vortex background. Near $f=0$, this is consistent with the observation that at $\tau = 0.5$ ($T = 3.27$ K), the temperature at which the impedance measurements reported below were performed, the escape probability $I_0^{-2}(\Delta/2kT)$ of a single vortex over the potential-energy barrier $\Delta(T) = 0.043E_J(T)$ opposing its motion in a triangular JJA [8] is very close to 1 [$I_0^{-2}(0.043/2\tau) = 0.999$, $I_0(x)$ is the modified Bessel function of order zero]. In the following, we focus on the central ($f=0$) quantum structures in $R(f)$ and $L(f)$ and study in detail how they evolve with frequency in the pinning-free regime at $\tau = 0.5$. Notice that, since τ is appreciably lower than $\tau_{KT} \approx 1.5$, effects due to thermally nucleated free vortices can be ignored.

Real and imaginary parts of $Z(f)$ measured at three different frequencies in a narrow range ($|f| < 0.05$) of frustrations centered about $f=0$ are shown in Fig. 2. Surprisingly, if f is not too small, $R(f)$ increases with ω, reaching saturation only near the upper limit of our spectral range. This is clearly inconsistent with the frequency independent flux-flow prediction $R(f) \approx R_n f$ for free vortices (R_n is the normal-state sheet resistance). Moreover, with decreasing frequency $R(f)$ and, in a more limited interval ($|f| < 0.005$, see inset), $L(f)$ exhibit growing negative curvature resulting in appreciable deviations from linearity. This shows that, even in the absence of pinning, vortex correlations are important, presumably because of the long-range logarithmic interaction be-

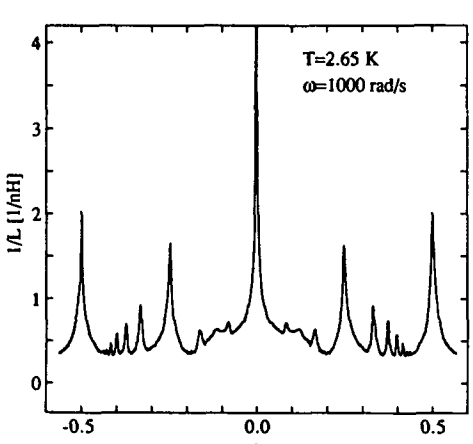

FIG. 1. Inverse sheet inductance of the triangular Josephson junction array as a function of frustration. See text for peak assignment to rational values of f.

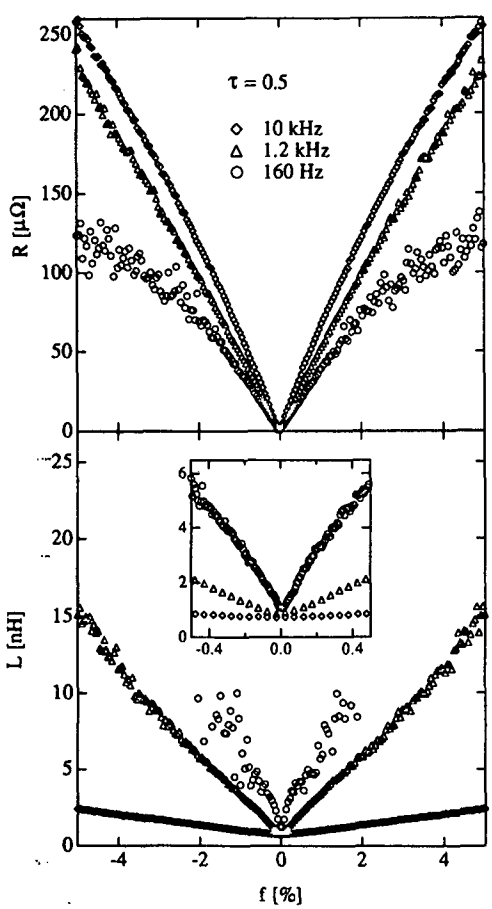

FIG. 2. Sheet resistance and sheet inductance of the triangular JJA at three different frequencies as a function of frustration in the range $|f| < 0.05$. The inset shows the $L(f)$ data in the interval $|f| < 0.005$.

tween the vortices. Notice, however, that $R(f)$ becomes linear and almost independent of ω in the limit $f \to 0$, as one expects for a plasma of noninteracting free vortices.

Deeper insight into this unexpected behavior is provided by an analysis of the impedance data near $f=0$ in terms of a complex dielectric constant $\varepsilon(\omega,f)$ defined by $Z(\omega,f)=i\omega L_k \varepsilon(\omega,f)$ [6,7]. According to Drude's prediction

$$\varepsilon(f,\omega)=1+2\pi(\sigma_0/i\omega) \tag{1}$$

for a 2D Coulomb plasma of free and independent vortices characterized by a *frequency independent* conductivity σ_0 proportional to the vortex density [9], i.e., $\sigma_0 \sim f$, $\varepsilon(\omega,f)$ is expected to be a function of f/ω only. Using $L_k(\tau=0.5)=0.69$ nH, the superfluid component $\mathrm{Re}(1/\varepsilon)$, which is the dynamical analog of the helicity modulus [2], and the dissipative component $\mathrm{Im}(1/\varepsilon)$ of $1/\varepsilon$ were inferred from a collection of impedance data taken at four different frequencies in the range $|f|<0.05$. The results are shown in Fig. 3 as a function of f/ω on a log-log plot. Within experimental accuracy [scattering of the data at large f/ω values arises from the extreme sharpness of the $f=0$ structure in $L(f)$ at the lowest driving frequencies], scaling of the data with f/ω is indeed observed over more than four decades in f/ω.

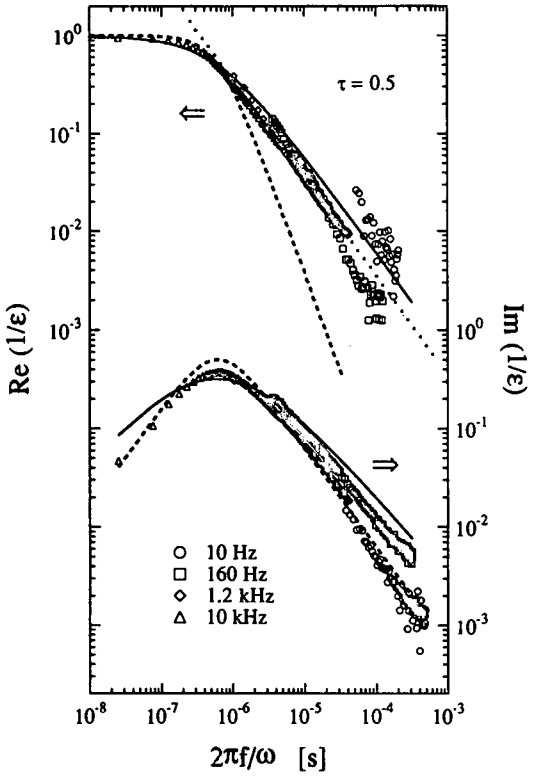

FIG. 3. Real and imaginary parts of the inverse complex vortex dielectric constant vs ratio of frustration to frequency on a log-log plot. Solid curve: Minnhagen's model; dashed curve: Drude's model; dotted straight line: $(f/\omega)^{-1}$ fit to the $\mathrm{Re}(1/\varepsilon)$ data at large f/ω values.

However, the log-log plot immediately reveals that, at large values of f/ω, $\mathrm{Re}(1/\varepsilon)$ scales as $(f/\omega)^{-1}$, in striking contrast to the $(f/\omega)^{-2}$ dependence predicted by Eq. (1). This unusual response of the vortex medium at low frequencies implies that $\mathrm{Re}(1/\varepsilon)$ is nonanalytical at $\omega=0$, thereby pointing to anomalous vortex diffusion. To see this in more detail, we begin by noticing that the functional dependence on f/ω emerging from the $\mathrm{Re}(1/\varepsilon)$ data of Fig. 3 can be described, to a first approximation, by an expression of the form

$$\mathrm{Re}(1/\varepsilon)=[1+(\omega_0/\omega)]^{-1}, \tag{2}$$

where ω_0 is an as yet unspecified characteristic frequency proportional to f. We pretend Eq. (2) is rigorous only at low frequencies ($\omega \ll \omega_0$) and provides a reasonable extrapolation to high frequencies. Recalling that $\mathrm{Im}(1/\varepsilon)$ is related to $\mathrm{Re}(1/\varepsilon)$ by a Kramers-Kronig relation, it follows [2] that

$$\mathrm{Im}(1/\varepsilon)=(2/\pi)(\omega_0/\omega)\ln(\omega_0/\omega)/[(\omega_0/\omega)^2-1]. \tag{3}$$

It is then straightforward to show that $\varepsilon(f/\omega)$, as given by Eqs. (2) and (3), can be cast into the Drude form Eq. (1), however, with σ_0 replaced by a *frequency dependent* complex vortex conductivity $\sigma_v(\omega)$. Expressing $\sigma_v(\omega)$ in terms of the vortex charge $q_v=(\pi E_J)^{1/2}$ [1,2], of the areal vortex density $n_v=4f/(a^2\sqrt{3})$ and of the complex vortex mobility $\mu_v(\omega)$ as $\sigma_v(\omega)=q_v^2\mu_v(\omega)n_v$, we find at low frequencies ($\omega \ll \omega_0$)

$$\mu_v(f/\omega)=(\pi/2)\mu_0[1+i(\pi/2)/\ln(\omega_0/\omega)]/\ln(\omega_0/\omega), \tag{4}$$

where $\mu_0=\omega_0/2\pi q_v^2 n_v$ is the (constant) mobility of an isolated vortex. Thus, the nonconventional scaling properties of $\varepsilon(f/\omega)$ imply that, for a given f, $\mu_v(\omega)$ vanishes as $1/|\ln\omega|$ in the limit $\omega \to 0$, thereby showing that vortex diffusion becomes anomalously slow (or "sluggish") at large time scales. In view of the fact that this remarkable feature emerges from the study of a pinning-free system, we believe it to be a general intrinsic property of ideal 2D superconductors, an interpretation corroborated by recent simulations [10] of the dynamics of thermally nucleated free vortices above T_{KT} in square arrays at zero frustration.

Additional evidence for anomalous vortex diffusion is provided by a quantitative analysis of the data of Fig. 3 based on Eqs. (2) and (3). Using the Bardeen-Stephen relation $\mu_0 \approx R_n a^2/\phi_0^2$ appropriate for arrays [6,8,12], we find $\omega_0=C(2/\sqrt{3})(2\pi/\phi_0)^2 R_n(kT/\tau)f$, where the numerical factor C, the only adjustable parameter of the model, is expected to be somewhat larger than 1. With this expression for ω_0, Eqs. (2) and (3) become identical to those obtained by Minnhagen [2] in his phenomenological treatment of Coulomb-gas dynamics. Using $R_n=2$ mΩ, as inferred from resistive measurements, and $C=5.45$ to fit the position of the maximum in $\mathrm{Im}(1/\varepsilon)$ at $\omega=\omega_0$, we find (see Fig. 3) that Minnhagen's approach provides a good description of $\mathrm{Re}(1/\varepsilon)$ and, with the exception of

the high-frequency range ($\omega \gg \omega_0$) where the model predictions are expected to be less accurate, also of $\mathrm{Im}(1/\varepsilon)$. For comparison, in Fig. 3 we also show the result of a calculation based on Drude's model [Eq. (1)]. Notice that, if the impedance is expressed as $Z \approx \phi_0^2 \mu_v n_v$ [12], Eq. (4) qualitatively accounts for the frequency dependence of the impedance data of Fig. 2, in particular for the weak negative curvature observed at low frequencies.

At the present level of understanding, we can only speculate about the nature of the microscopic mechanisms responsible for sluggish vortex motion. It is well known that diffusion in disordered systems does not obey the classical laws thereby leading to anomalous transport properties [13]. However, on account of the extreme uniformity of the array emerging from Fig. 1, we exclude disorder-induced pinning as a possible source of anomalous vortex diffusion. The key feature of randomness needed to explain the *nonanalytic* behavior of $1/\varepsilon$ would be some very peculiar hierarchical distribution of energy barriers [13], a requirement difficult to reconcile with the exceptional richness of the fine structure of $Z(f)$. The only conceivable pinning mechanism operating in our system at $\tau = -0.5$ is edge pinning [12] due to the finite size of the sample, but it appears to be unlikely that size effects could significantly affect vortex dynamics in experiments relying on the two-coil technique [4]. A more plausible mechanism which could intrinsically reduce the vortex mobility at low frequencies results from the coupling of the vortices to the 2D acoustic modes (the spin-wave excitations of the XY model) of the phases associated with the superconducting islands of the array. This mechanism has been studied in detail in connection with the dissipation generated by moving "massive" vortices in the quantum regime [14], but it should also be relevant to determine the friction of massless vortices in the overdamped classical regime studied in this work. In particular, it reproduces the low-frequency behavior $\mu_v(\omega) \sim 1/|\ln\omega|$ in two dimensions [15]. Moreover, if one takes into account vortex correlations through a liquidlike vortex structure factor with a main peak at a wave number related to the mean vortex distance, this model also predicts the scaling of μ_v with f/ω, thereby providing an explanation of the nonlinearity of $Z(f)$ shown in Fig. 2.

In conclusion, ac impedance measurements performed over a wide range of frequencies on an almost pinning-free triangular array of Josephson junctions exposed to a weak magnetic field have disclosed novel and unexpected features of vortex dynamics in an ideal two-dimensional superconductor. Our analysis in terms of a complex vortex dielectric constant implies that, in striking contrast with Drude's classical prediction for a two-dimensional Coulomb gas of free and independent vortex charges, the vortex mobility vanishes logarithmically in the limit of small frequencies, thereby pointing to anomalous vortex diffusion.

We would like to thank S. E. Korshunov for very stimulating discussions and B. Jeanneret and R. Meyer for their assistance in the analysis of the data. This work was supported by the Swiss National Science Foundation.

[1] J. M. Kosterlitz and D. J. Thouless, J. Phys. C **6**, 1181 (1973).
[2] P. Minnhagen, Rev. Mod. Phys. **59**, 1001 (1987).
[3] D. J. Bishop and J. D. Reppy, Phys. Rev. B **22**, 5171 (1980).
[4] A. T. Fiory, A. F. Hebard, P. M. Mankiewich, and R. E. Howard, Appl. Phys. Lett. **52**, 2165 (1988); B. Jeanneret, J. L. Gavilano, G. A. Racine, Ch. Leemann, and P. Martinoli, Appl. Phys. Lett. **55**, 2336 (1989).
[5] A. F. Hebard and A. T. Fiory, Phys. Rev. Lett. **44**, 291 (1980).
[6] Ch. Leemann, Ph. Lerch, G. A. Racine, and P. Martinoli, Phys. Rev. Lett. **56**, 1291 (1986).
[7] A. T. Fiory and A. F. Hebard, Phys. Rev. B **25**, 2073 (1982).
[8] C. J. Lobb, D. W. Abraham, and M. Tinkham, Phys. Rev. B **27**, 150 (1983).
[9] V. Ambegaokar, B. I. Halperin, D. R. Nelson, and E. D. Siggia, Phys. Rev. B **21**, 1806 (1980); S. R. Shenoy, J. Phys. C **18**, 5163 (1985).
[10] P. Minnhagen and O. Westman (unpublished).
[11] R. Théron, J. B. Simond, J. L. Gavilano, Ch. Leemann, and P. Martinoli, Physica (Amsterdam) **165&166B**, 1641 (1990).
[12] M. S. Rzchowski, S. P. Benz, M. Tinkham, and C. J. Lobb, Phys. Rev. B **42**, 2041 (1990); H. S. J. van der Zant, H. A. Rijken, and J. E. Mooij, J. Low Temp. Phys. **82**, 67 (1991).
[13] S. Havlin and D. Ben-Avraham, Adv. Phys. **36**, 695 (1987).
[14] U. Eckern and A. Schmid, Phys. Rev. B **39**, 6441 (1989).
[15] H. Beck (unpublished).

Physica Scripta. Vol. T49, 176–179, 1993

Superconducting Vortices in Triangular and Square Josephson Junction Arrays

P. Martinoli, R. Theron, J.-B. Simond, R. Meyer, Y. Jaccard and Ch. Leemann

Institut de Physique, Université de Neuchâtel, 2000 Neuchâtel, Switzerland

Received March 29, 1993; accepted April 2, 1993

Abstract

Experiments probing vortex dynamics in square and triangular Superconducting–Normal–Superconducting Josephson junction arrays are reviewed. A low frequency two coil mutual inductance technique allows to investigate phase coherence in these samples. In a perpendicular magnetic field the interaction of the field induced vortices with the periodic pinning structure provided by the array leads to frustration effects which, interestingly enough, differ in the two types of arrays. This difference in behavior is mainly due to the smaller pinning energy in the triangular array.

1. Introduction

The classical XY model consists of a regular lattice of spins on the XY-plane, subject to nearest neighbor interactions and free to rotate about an axis perpendicular to the XY-plane. Each spin is described by the angle ϕ_i which it makes with an arbitrary, fixed reference direction. According to conventional wisdom [1], there exists no long range order in such a system at all physically reasonable temperatures, there can thus be no solid–liquid (long range order to short range order) phase transition. There exists, however, at low temperatures, an intermediate type of order, characterized by an algebraically decaying spin–spin correlation function and therefore a new type of phase transition to the high temperature short range order (exponentially decaying correlation function). The Kosterlitz–Thouless (KT) phase transition [2] is characterized by the creation, in the spin landscape, of thermally excited topological defects (vortex–antivortex pairs) close to but below the transition temperature, and the creation of free vortices at and above the transition temperature.

Josephson junction arrays are a, perhaps the only, almost perfect physical realization of the XY model. These arrays consist of superconducting islands at the sites of a regular lattice, weakly coupled through Josephson junctions with the nearest neighbors. In the present work, we will *assume* a sinusoidal current–phase relation. Then, if the magnitude of the superconducting order parameter $\Psi_j = \Psi_0 \exp(i\phi_j)$ is constant everywhere, indeed, an array is isomorphic to the XY model with the naïve phase of the superconducting order parameter playing the role of the spin. The gauge invariant phase difference between two neighboring islands (going from i to j) is given by

$$\Delta\Phi_{ij} = \phi_j - \phi_i + \frac{2\pi}{\Phi_0}\int_i^j A \cdot \mathrm{d}x \qquad (1)$$

where A is the magnetic vector potential. The supercurrent i_s flowing through the junction (from j to i) is then given by a Josephson equation $i_s = i_c \sin \Delta\Phi_{ij}$ where i_c is the junction critical current. In a dissipative state the voltage $V \equiv V_j - V_i$ across our junction will be given by the second Josephson equation $2eV = \hbar\,(\mathrm{d}/\mathrm{d}t)(\Delta\Phi_{ij})$. From the two Josephson relations one can deduce the junction's coupling energy

$$E = -E_j \cos \Delta\Phi_{ij} \qquad (2)$$

with $E_J = \hbar i_c/(2e)$. The Hamiltonian of our array is thus

$$H = -E_J \sum_{\langle ij \rangle} \cos \Delta\Phi_{ij} \qquad (3)$$

where the sum is over all pairs. Equation (3) explicitly shows the relationship between array and XY model. In a magnetic field the vector potential modifies the coupling so that for some pairs it changes from *ferro-* to *antiferro*-magnetic: the frustrated XY model. Notice also the temperature dependence, through i_c, of the coupling constant, which justifies the introduction of a reduced temperature $\tau = 2ek_B T/(\hbar i_c)$. As an example of frustration, let us consider [3] a square array at full frustration: $f = \frac{1}{2}$, the frustration parameter f denoting the applied magnetic field in numbers of flux quanta per unit cell of the array. If, for a magnetic field along the z-direction, the vector potential is expressed as $A_y = H_z x$, then it is easy to see, using eq. (1), that the contribution of the vector potential to the change in phase is zero along all horizontal bonds and alternatively zero and π along the vertical bonds, rendering these last ones antiferromagnetic. The situation is shown in Fig. 1(a), the thick lines representing the antiferromagnetic bonds and leading

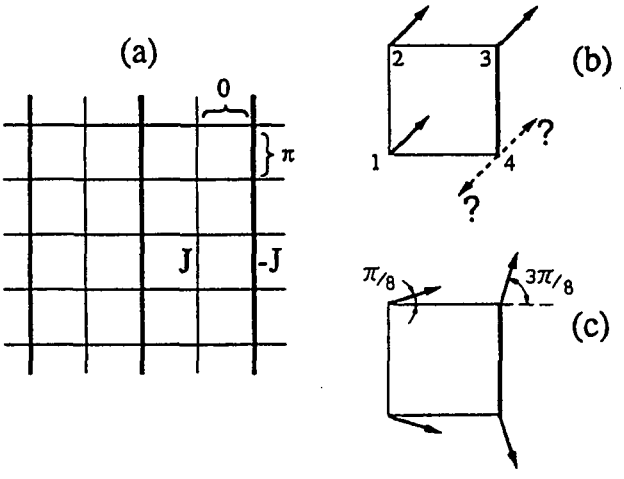

Fig. 1. The fully frustrated case $f = \frac{1}{2}$ in a square array [3]. In (a) the contribution of the vector potential to the gauge invariant phase is π along the fat bonds (rendering them antiferromagnetic), 0 along the skinny bonds (ferromagnetic). The resulting frustration (b) leads to the phases ϕ_j drawn in (c).

to the "frustration" depicted in Fig. 1(b) for the spin at position 4. The resulting ground state configuration is shown in Fig. 1(c).

In general there are two contributions to the magnetic vector potential: from the magnetic field, as above, and from the screening currents in the array, a contribution which we will neglect here. In this weak screening limit $\oint A \cdot dx = \Phi_0 f$, and fluxoid quantization leads to $\sum \Delta\Phi_{ij} = 2\pi(m + f)$ where the sum is over the links in one unit cell and m is the number of vortices assigned to the cell. The ground state for the ϕ_j is determined by minimizing the free energy under the constraints imposed by Kirchhoff's laws at every lattice site: a formidable problem, which so far has been solved only for special values of the magnetic field. A useful hint: when actually performing this sum, do not forget to ensure that $-\pi < \phi_j \leqslant +\pi$.

2. The experiments

The samples were produced using standard evaporation techniques and photolithography [4]. The triangular array considered below was patterned from a Cu/Pb bilayer (both layers approximately 300 nm thick) on a sapphire substrate. The Pb islands, in the form of six-armed stars, formed a triangular lattice of lattice parameter $a = 15\,\mu m$, the gap between two adjacent arms was $l = 1\,\mu m$. The precise value of l is not very critical, however the critical current from one Pb arm, through the Cu, to the neighboring Pb arm and thus the coupling energy of this superconducting–normal–superconducting (SNS) junction, are proportional to $\exp(-l/\xi_n)$, where ξ_n is the normal metal coherence length, typically ~ 100 nm in our experiments. A small variation in l can therefore lead to large changes in E_J across the array. Given a good Cu/Pb interface, the most critical parameters in the array production process are thus: uniformity of the light exposing the photoresist, the photoresist developing process and, finally, a gentle and uniform ion beam milling.

The complex a.c. conductance of the sample as a function of temperature and magnetic field was measured with the two coil mutual inductance technique described by Jeanneret *et al.* [5]. The signal from the (superconducting) gradiometer detection coil was measured with an rf SQUID in the flux-locked loop mode and the SQUID output fed into a phase-sensitive detector. The high sensitivity of this measurement system allowed to explore the low drive current I_D (typically $\sim 0.1\,\mu A$, corresponding to $10^{-4}\Phi_0$ per unit cell), low angular frequency ω [down to $\omega/(2\pi) \sim 10$ Hz] region in parameter space.

As an example, the imaginary and the real part of the measured signal normalized to V_{ss}, the low temperature full screening value of the imaginary part, as a function of magnetic field in units of f is shown in Fig. 2. Comparing this measurement with the magnetoconductance of square, but otherwise similar arrays [6], two striking differences are immediately noticed: the triangular array exhibits an even richer structure – in addition to the low order structures predicted by theory ($f = \frac{1}{2}, \frac{1}{3}, \frac{1}{4}$), peaks at high order rational f-values such as odd multiples of $f = \frac{1}{12}$ are also resolved – and the peaks of Fig. 2 are much narrower than the ones observed in a square array. While the first feature could be due to a better sample homogeneity and/or to the much smaller (two orders of magnitude) drive current, a careful analysis has shown that the sharpness of the peaks is an intrinsic characteristic of triangular arrays. Eventually, this extreme sensitivity of our array to small changes in the applied magnetic field has forced us to install a superconducting solenoid equipped with a persistent switch and to achieve excursions of the magnetic field around a fixed value with a flux pump.

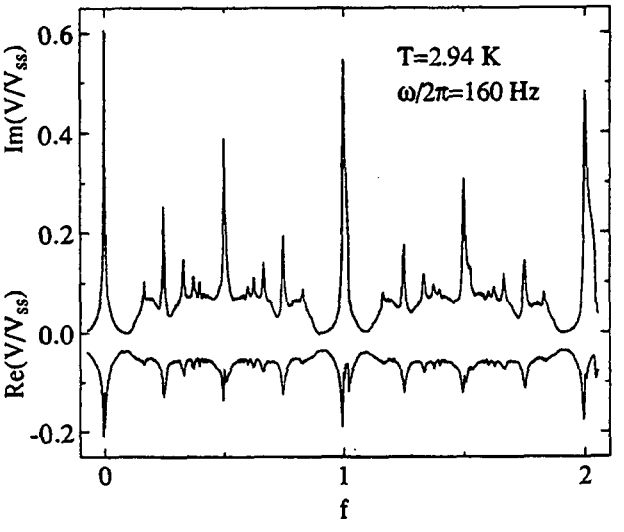

Fig. 2. Real and imaginary parts of the measured signal, normalized to V_{ss}, as a function of frustration.

3. Results and discussion

In our experiments we measure the sample's complex sheet impedance $Z = R + i\omega L$. On the other hand, when performing Monte Carlo calculations, the results are typically expressed in terms of a quantity called helicity modulus Γ, corresponding to the free energy increment associated with a change $\phi_i \to \phi_i + \delta\phi_i$ in the phases of the order parameter. Originally [7], Γ was introduced as a scalar, proportional to the superfluid density. It is then an easy matter to show that

$$\Gamma = \left(\frac{\Phi_0}{2\pi}\right)^2 \frac{1}{L} \tag{4}$$

Subsequently [8, 9] it became clear that the helicity modulus needs to be correctly treated as a tensor, in general the relationship between Γ and directly accessible experimental quantities is thus by no means trivial, even though it was conjectured in Ref. [9] that $\Gamma_{\alpha\beta}$ is proportional to the corresponding imaginary part of the a.c. conductivity. Fortunately, it turns out [10] that for 2D regular arrays $\Gamma = \Gamma \cdot \mathbf{I}$ where $\mathbf{I}$ is the 2×2 unit tensor, so that the use of eq. (4) is certainly justified in the present context.

It is instructive to notice that an equivalent way to calculate Γ for the $T = 0$ ground state is to define, via the Josephson equations, the single junction inductances $L_{ij} = V_{ij}/(dI_{ij}/dt)$ and therefore $L_{ij}^{-1} = L_J^{-1} \cdot \cos(\Delta\Phi_{ij})$ with $L_J = (\Phi_0/2\pi)^2/E_J$. Then the helicity modulus may be determined by adding up the individual inductances to obtain the inverse array sheet inductance [11].

In Figs 3 and 4 we compare the helicity modulus for triangular and square lattices. For a square SNS array the helicity modulus as a function of reduced temperature in zero magnetic field and at full frustration is shown in Fig. 3. Notice that there is a truly excellent agreement between the measurement and the Monte Carlo simulation [12], espe-

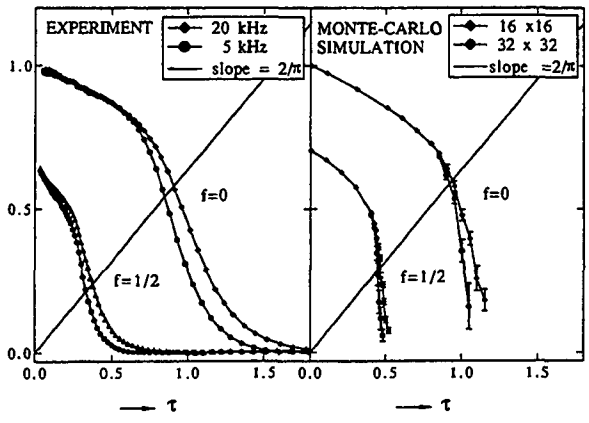

Fig. 3. The helicity modulus, in units of E_J, of a square array as a function of reduced temperature at $f = 0$ and $f = \frac{1}{2}$ as determined by experiment (a) and with a Monte Carlo simulation [12] (b). The diagonal line of slope $2/\pi$ is the universal KT prediction for the transition temperature which is seen to correspond approximately to the low temperature end of the steep sections.

cially since there are no adjustable parameters! The diagonal line of slope $2/\pi$, representing the KT universal prediction for the phase transition, correctly predicts the transition temperature for both, the $f = 0$ and $f = \frac{1}{2}$, curves. As the measuring frequency ω increases, the probing length being proportional to $\omega^{-1/2}$ [13], the measured signal stems from smaller vortex pairs and the transition shifts to slightly higher temperatures, again in agreement with the Monte Carlo calculations for the smaller array. No evidence is seen for an Ising-type transition related to a degeneracy of the ground state at $f = \frac{1}{2}$ [14], thereby confirming our previously published result [15] that the mechanism responsible for the transition at $f = \frac{1}{2}$ is vortex unbinding, just as at $f = 0$.

The helicity modulus as a function of reduced temperature at $f = 0$ and $f = \frac{1}{2}$ for the triangular array is shown in Fig. 4(a) and 4(b). The agreement with the corresponding Monte Carlo simulations [16] is good only for the extrapolated zero temperature value of the helicity modulus. In both cases the measured transition temperatures are distinctly lower than the KT prediction or the results of the simulations (these last ones being $\tau_c \simeq 1.5$ at $f = 0$ and $\tau_c \simeq 0.5$ at $f = \frac{1}{2}$). A very small detuning of the frustration, $\delta f \simeq 10^{-4}$, results in an overall reduction of the helicity modulus. This effect indicates a possible explanation for the

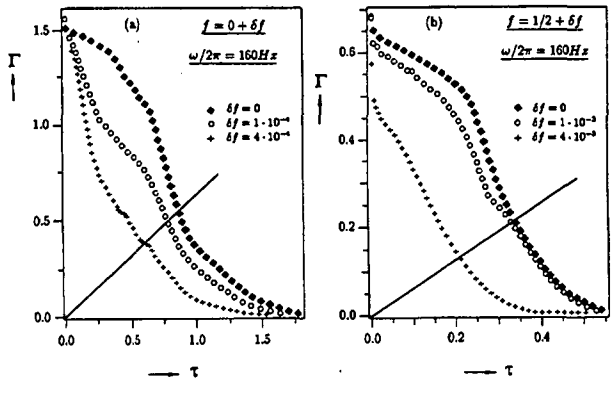

Fig. 4. The helicity modulus, in units of E_J, of a triangular array as a function of reduced temperature at $f = 0 + \delta f$ (a) and $f = \frac{1}{2} + \delta f$ (b). The measured transition temperatures are seen to be lower than the KT prediction (diagonal line of slope $2/\pi$).

discrepancy between experiment and theory: even the "perfectly" tuned field values are in reality slightly detuned. Aside from operator error, this could be due to the influence of the screening currents which may not be negligible in the whole temperature range considered. The reason why this effect was not observed in the result for the square array (Fig. 3 above) is that the energy necessary for a vortex to cross the energy barrier opposing its motion is approximately 5 times larger in the square array than in the triangular array [17]. When computing the vortex mobility, this factor of 5 appears in the argument of I_0, a modified Bessel function of order zero, leading to a very much larger mobility already at relatively low temperatures in the triangular case. Since in addition the theoretically predicted reduced transition temperature is larger for the triangular array, it is not surprising anymore that the true transition is masked by the presence of spurious, highly mobile vortices.

The validity of the above interpretation is confirmed by the results reported in Fig. 5(a) and 5(b), where the temperature and frequency evolution of the inverse sheet inductance as a function of frustration is shown. The peaks in L^{-1} quite clearly sharpen up with increasing temperature and decreasing measuring frequency, to approach, on a scale $0 \leqslant f \leqslant \frac{1}{2}$, the sharpness of a delta-function at the highest temperature and smallest frequency. Both of these features are due to the high vortex mobility in the triangular array: while the magnetic field vortices corresponding to high order rational f-values are pinned, any deviation from the

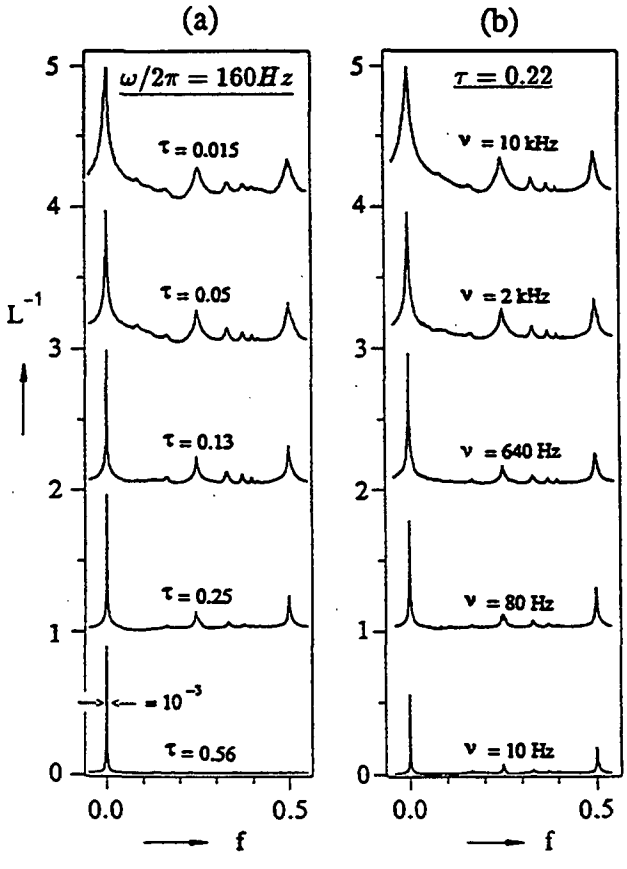

Fig. 5. Inverse sheet inductance, normalized to the low temperature saturation value, of a triangular array as a function of frustration. In (a) the excitation frequency is kept constant while the temperature increases from top to bottom. In (b) the temperature is constant and the measuring frequency decreases from top to bottom. Successive curves are displaced by unity along the vertical axis.

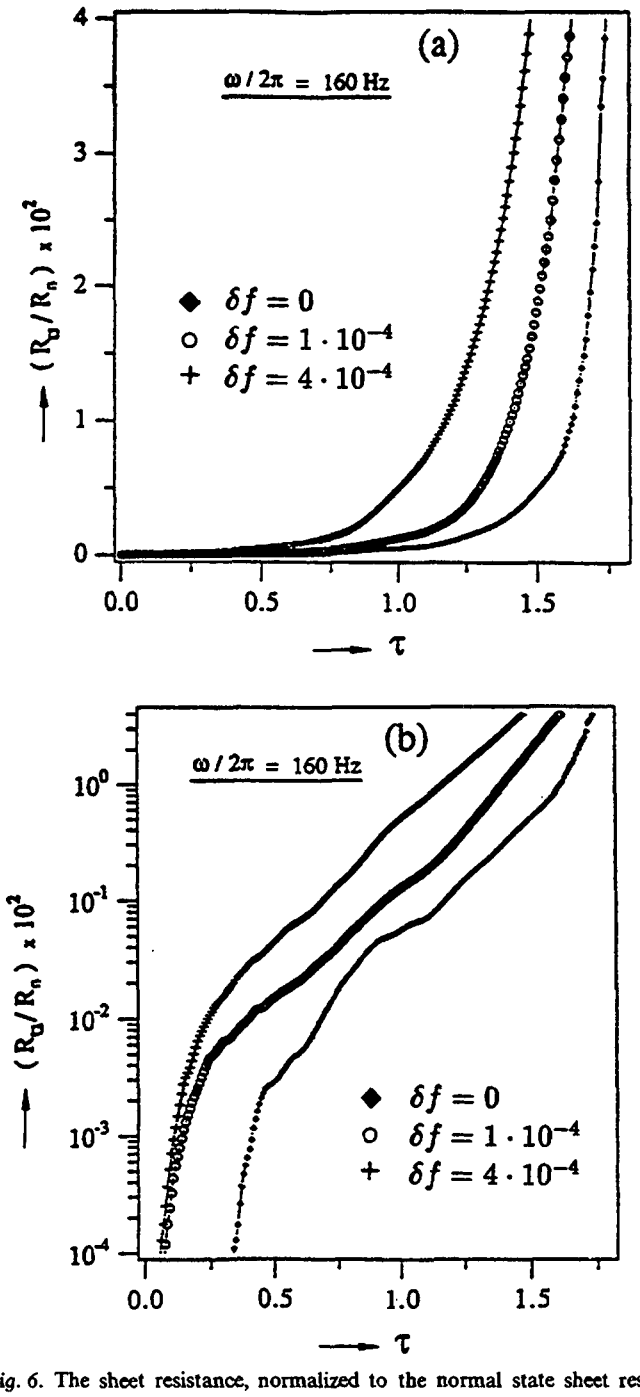

Fig. 6. The sheet resistance, normalized to the normal state sheet resistance, of a triangular array as a function of reduced temperature at $f = 0 + \delta f$ on a linear (a) and on a logarithmic scale (b).

peaks introduces highly mobile vortex lattice defects. With increasing temperatures it is the increasing vortex mobility (and, to a smaller extent, the thermal excitations) which produces large dissipation, i.e. a sizeable reduction in superfluid density as soon as the magnetic field deviates from a peak value.

On the other hand, as the frequency of the excitation current decreases, the probing length increases (a larger section of the sample is observed) [13], meaning that for a given deviation from a peak, the number of mobile vortices observed increases.

As a conclusion, we present in Fig. 6(a) and 6(b) the sheet resistance of the triangular array as a function of reduced temperature at $f = 0 + \delta f$ with $\delta f = 0$, 10^{-4} and 4×10^{-4}. In Fig. 6(a) the scale on the ordinate is linear and the resistance appears to explode at $\tau_c \simeq 1.5$, which is the correct transition temperature for a KT transition [16]. On a logarithmic scale [Fig. 6(b)] this feature almost disappears, to be replaced by a puzzle at the low temperature end. While the $f = 0$ curve seems to approach zero resistance at a non-zero temperature, one gets the impression that the slightly detuned curves indicate the presence of dissipation down to zero temperature, opening up the question of the existence and nature of superconductivity in an incommensurate state (f approaching an irrational value). This problem will be addressed hopefully soon in a separate publication [18].

Acknowledgements

Interesting discussions with S. E. Korshunov are gratefully acknowledged. This work was supported by the Swiss National Science Foundation.

References

1. Ashcroft, N. W. and Mermin, N. D., "Solid State Physics" (Saunders, Philadelphia 1976).
2. Kosterlitz, J. M. and Thouless, D. J., J. Phys. C6, 1181 (1973).
3. Halsey, T. C., J. Phys. C18, 2437 (1985).
4. Lerch, Ph., Theron, R., Leemann, Ch. and Martinoli, P., IEEE Trans. Magn. MAG-23, 1126 (1987).
5. Jeanneret, B. *et al.*, Appl. Phys. Lett. 55, 2336 (1989).
6. Leeman, Ch., Lerch, Ph., Racine, G.-A. and Martinoli, P., Phys. Rev. Lett. 56, 1291 (1986).
7. Fisher, M. E., Barber, M. N. and Jasnow, D., Phys. Rev. A8, 1111 (1973).
8. Ohta, T. and Jasnow, D., Phys. Rev. B20, 139 (1979).
9. Shih, W. Y., Ebner, C. and Stroud, D., Phys. Rev. B30, 134 (1984).
10. Shih, W. Y. and Stroud, D., Phys. Rev. B30, 6774 (1984).
11. Martinoli, P., unpublished result.
12. Teitel, S. and Jayaprakash, C., Phys. Rev. B27, 598 (1983).
13. Shenoy, S. R., J. Phys. C18, 5163 (1985); Ambegaokar, V., Halperin, B. I., Nelson, D. R. and Siggia, E. D., Phys. Rev. B21, 1806 (1980).
14. Lee, D. H., Joannopoulos, J. D., Negele, J. W. and Landau, D. P., Phys. Rev. B33, 450 (1986).
15. Lerch, Ph., Leemann, Ch., Theron, R. and Martinoli, P., Phys. Rev. B41, 11579 (1990).
16. Shih, W. Y. and Stroud, D., Phys. Rev. B32, 158 (1985).
17. Lobb, C. J., Abraham, D. W. and Tinkham, M., Phys. Rev. B27, 150 (1983).
18. Martinoli, P. *et al.*, to be published.

Dynamics of the phase transition in proximity-effect arrays of Josephson junctions at full frustration

Ph. Lerch, Ch. Leemann, R. Theron, and P. Martinoli
Institut de Physique, Université de Neuchâtel, 2000 Neuchâtel, Switzerland
(Received 27 December 1989)

With a mutual-inductance method the effective kinetic inductance of square arrays of 10^6 proximity-effect Pb-Cu-Pb Josephson junctions was measured. The magnetic field was tuned to achieve full frustration $f=\frac{1}{2}$, the frustration parameter $f\equiv\Phi/\phi_0$ being the ratio of the applied magnetic flux Φ per unit cell of the array and the superconducting flux quantum ϕ_0. A test of the temperature dependence of the free vortex correlation length as well as of the helicity modulus was performed and found to be consistent with a description of the phase transition at $f=\frac{1}{2}$ within the framework of the Kosterlitz-Thouless-Berezinski ideas. The results do not, however, provide information concerning the possible presence of an Ising-like transition, which may exist in the fully frustrated case.

Under certain conditions regular two-dimensional (2D) arrays of Josephson junctions map onto the planar XY model,[1] allowing intense feedback between theoretical models and physical reality, and providing convenient model systems for the study of a number of concepts such as renormalization, scaling, frustration, commensurability, and randomness. In a perpendicular magnetic field, the array's behavior is dominated by the commensurability (or lack thereof) between the applied vortex lattice and the array lattice, resulting in a periodic modulation of the $T_c(H)$ phase boundary.[2-9] In terms of the frustration parameter f, the number of applied flux quanta per unit cell of the array, the periodicity of the phase boundary is $\Delta f=1$. Strong structures appear at integer values of f and smaller structures at some rational f values; their relative amplitude being mainly determined by lattice topology.[3] At integer f values, the phase transition has been shown to be of the Kosterlitz-Thouless-Berezinski (KTB) type.[3,5,10] In the fully frustrated $f=\frac{1}{2}$ case the two possible ground states have the same energy, but opposite chirality.[10] The nature of the phase transition at $f=\frac{1}{2}$ is thus additionally complicated by the possible existence of an Ising-type transition related to the discrete chiral symmetry.[11] This transition at T_I is characterized by a proliferation of domain walls which are expected to lead to additional dissipation.[9]

The present paper reports an investigation of the superconducting transition of proximity-effect Josephson arrays at full frustration. Our measurements provide a clear demonstration that the underlying mechanism relevant at the transition is vortex unbinding.

In order to investigate the nature of the transition to a phase-ordered superconducting state in 2D, we have produced, using standard photolithography and ion milling, square arrays of $\sim 10^6$ square lead islands on top of a copper layer. The lattice parameter was $a=8$ μm, the length of the (weak) copper link between two adjoining lead islands 1.7 μm.[12] At temperatures well below T_{cs}, the transition temperature of the lead islands, the phase ϕ_i of the superconducting order parameter describes the state of each island and takes the role of the spin angle variable in the XY model. Since the coupling constant $J=\hbar i_c(T)/(2e)$, where i_c is the single junction critical current in the absence of fluctuations, is temperature dependent, the link between the XY model and the array is effected by introducing a reduced temperature $\tilde{T}$ defined by $\tilde{T}=k_BT/J(T)$. A precise determination of i_c is thus crucial to investigate renormalization effects due to collective behavior. At temperatures low enough to exclude the presence of critical 2D fluctuation effects, measurements of the critical current of the whole array, divided by the appropriate number of junctions, were fitted to the expression $i_c(T)=i_{c0}(1-T/T_{cs})^2\exp[-L/\xi_n(T)]$, where $\xi_n(T)$ is the dirty-limit normal-metal coherence length.[13] The values of i_c in the transition region were then calculated with this expression.

The dynamics of the phase ordering transition was studied with a variation[14] of the two coil technique devised by Hebard and Fiory:[15] an excitation coil induces screening currents in the film, which are related to the sample's complex conductance G. These screening currents induce a signal in the detection coil, which can be phase sensitively detected. In Fig. 1 we show the real $\mathrm{Re}(\delta V)$ and the quadrature $\mathrm{Im}(\delta V)$ components of the signal voltage as a function of temperature measured at $f=0$ and $f=\frac{1}{2}$. Except for an overall shift to lower temperatures in the $f=\frac{1}{2}$ case, the signals are quite similar, showing a peak in the $\mathrm{Re}(\delta V)$ component and a roll-off in the $\mathrm{Im}(\delta V)$ component of the signal voltage, which, for integer f values, have been shown to be the signatures of a KTB vortex-unbinding transition.[5] It appears, therefore, reasonable to attempt an analysis of the $f=\frac{1}{2}$ data within the framework of the KTB theory. Notice, nonetheless, that the peak in the $\mathrm{Re}(\delta V)$ component at $f=\frac{1}{2}$ is slightly wider than at $f=0$, showing evidence of additional dissipation which may be due to the presence of yet unidentified topological excitations.

In the dynamical extension of the KTB theory,[16,17] the description of the transition is in terms of a frequency-dependent complex dielectric constant $\epsilon(\omega,T)=\epsilon'+i\epsilon''$. From the measured voltage, G is extracted,[14,18] and related to $\epsilon(\omega,T)$ via $G^{-1}=i\omega L_k\epsilon(\omega,T)$,[19,20] where L_k

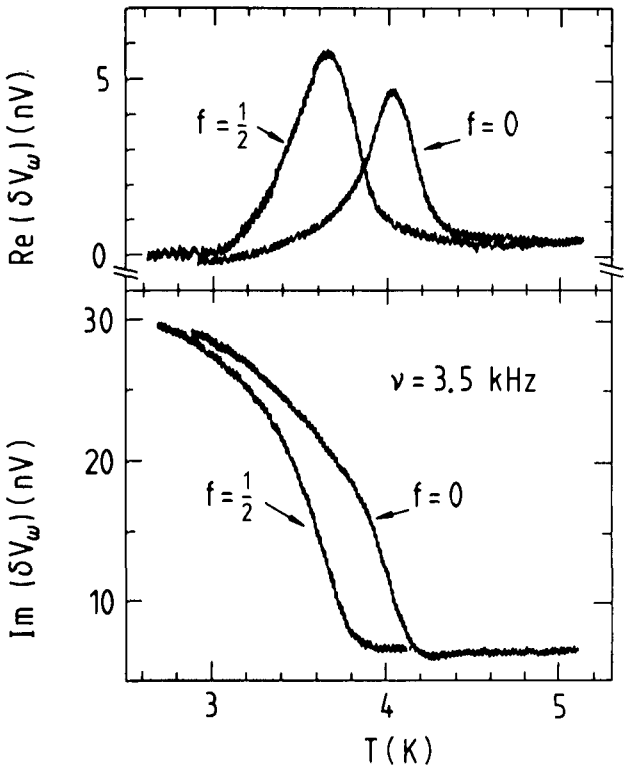

FIG. 1. Real $\mathrm{Re}(\delta V)$ and imaginary $\mathrm{Im}(\delta V)$ part of the detected voltage as a function of temperature in zero field and at full frustration.

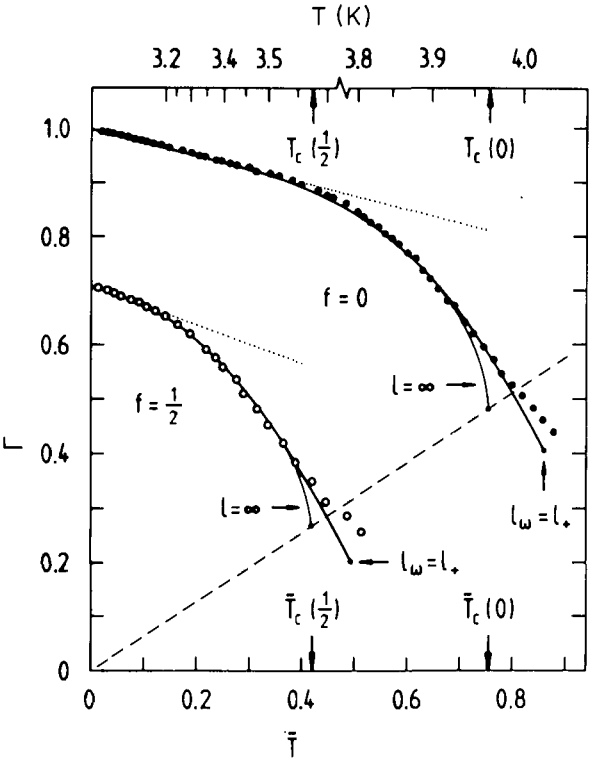

FIG. 2. Helicity modulus $\Gamma(\tilde{T})$ as a function of the reduced temperature $\tilde{T}$ for $f=0$ and $f=\frac{1}{2}$, at a measuring frequency of 8 kHz. The linear decrease at low temperatures (dotted lines) is caused by the spin waves. The solid lines are the results obtained from the KT scaling equations, the dashed line represents the universal jump in superfluid density predicted by Eq. (2).

$=\phi_0/[2\pi i_c(T)]$ is the bare kinetic inductance of the array.[21] The helicity modulus Γ, a measure of the phase order in the system, is given by[20,22,23]

$$\Gamma=\frac{F_{sw}}{\epsilon'(T)}, \tag{1}$$

where the term F_{sw} describes the depletion of order due to spin waves and is given by $1-\tilde{T}/4$ at $f=0$ (Ref. 22) and $(1-\tilde{T}/2)/\sqrt{2}$ at $f=\frac{1}{2}$.[23] In Fig. 2 $\Gamma(\tilde{T})$ for $f=0$ and $f=\frac{1}{2}$ is presented. The single junction critical current $i_{c,f=1/2}$, entering the definition of $\tilde{T}$ at $f=\frac{1}{2}$, was deduced from the array critical current $i_{c,A}$, measured at $f=\frac{1}{2}$ to take into account the weak magnetic field dependence of the single junction critical current, and fitted to the same expression as in the $f=0$ case. The resulting $i_{c,A}$ was then corrected by the factor calculated by Halsey[10] relating array and single junction critical current: $i_{c,f=1/2}=i_{c,A}/(\sqrt{2}-1)$. The low-temperature portion of the experimental points showing a linear decrease of Γ with increasing temperature is due to the *ad hoc* incorporation of the spin waves, whereas the drop at higher temperatures is due to the variation of the superfluid density near T_c. In the KTB picture, the transition temperature T_c, defined as the temperature at which vortex-antivortex pairs of infinite size unbind, is determined by the relation[24,25]

$$2k_BT_c=\frac{\pi J}{\epsilon_c}, \tag{2}$$

ϵ_c describing the amount of screening experienced by pairs of infinite size. The solid lines in Fig. 2 are results from a numerical solution of the KT scaling equations, the dashed line is the universal jump predicted by Eq. (2). The numerical solutions were calculated for infinite scale and for a scale $l=l_\omega\equiv\ln(r_\omega/a)$, where $r_\omega=\sqrt{14D/\omega}$ is, approximately, the size of the largest pairs responding to an ac field of angular frequency ω (Ref. 16) and D is the vortex diffusion constant. In the latter case the renormalization process is stopped when the free vortex correlation length $\xi^+=r_\omega$. There are two independent fitting parameters in the numerical procedure, ϵ_c and N_0, the number of configurations of a vortex-antivortex pair of size a in the system.[26] The critical temperature is defined by the intersection between the dashed line and Γ. The agreement between the numerical calculations and the experimental values is good up to T_c. At higher temperatures there is some divergence due to the strong rise of dissipation above T_c.

A further test of the validity of the description of our data within the framework of the KTB ideas is provided by a measure of the temperature dependence of ξ^+. Above T_c, ξ^+ is expected to have the following peculiar temperature dependence[24]

$$\xi^+(T)=c\exp[b(T-T_c)^{-1/2}], \tag{3}$$

where c is of the order of the lattice constant a and b a constant of order unity. An experimental verification of Eq. (3) (Ref. 5) is equivalent to a check of the relation-

ship $r_\omega = \xi^+(\tilde{T})$, which reduces to

$$l_\omega^{-2} = b^{-2}(\tilde{T}_\omega - \tilde{T}_c). \quad (4)$$

The T_ω values were deduced by extrapolating to zero the steep portions of the $\mathrm{Im}(\delta V)$ curves. The result of this procedure is shown in Fig. 3, from which we conclude that the free vortex correlation length has indeed the characteristic KTB temperature dependence predicted by Eq. (3). Notice that here the effect of the spin waves is included in the choice of the independent variable, $\tau = \tilde{T}/(1-\tilde{T}/4)$ at $f=0$ and $\tau = \tilde{T}/[\sqrt{2}(1-\tilde{T}/2)]$ at $f = \frac{1}{2}$.[23] Also, Eq. (3) is strictly valid only very close to T_c, it is thus somewhat surprising to find such good agreement in the investigated temperature range.

In the frequency dependence analysis (Fig. 3), the values obtained for the reduced critical temperatures are $\tilde{T}_c(f=0)=0.83$ and $\tilde{T}_c(f=\frac{1}{2})=0.36$. The Γ analysis (Fig. 2) yields $\tilde{T}_c(f=0)=0.75$ and $\tilde{T}_c(f=\frac{1}{2})=0.42$. The values for the dielectric constant at T_c are $\epsilon_c(f=0)=1.5$ and $\epsilon_c(f=\frac{1}{2})=2.5$ and $\epsilon_c(f=0)=1.69$ and $\epsilon_c(f=\frac{1}{2})=2.09$ as obtained from the analysis of Figs. 2 and 3, respectively. These numbers show that two completely different analyses exhibit roughly equal results. When compared with the results obtained by Teitel and Jayaprakash[3] with Monte Carlo (MC) simulations, the agreement is very satisfactory: they obtained $\tilde{T}_c(f=0)=0.91$ and $\tilde{T}_c(f=\frac{1}{2})=0.45$. More than the absolute numbers themselves, the ratio $\tilde{T}_c(f=0)/\tilde{T}_c(f=\frac{1}{2})$ obtained in our experiments is in almost perfect agreement with the MC results. In addition, a consistency test can be performed. The parameter b of Eq. (3) obtained from the ξ^+ analysis can be calculated using the $N_0(N_0=0.25$ at $f=0$ and $N_0=0.20$ at $f=\frac{1}{2})$ and ϵ_c values used in the fit for the Γ data.[26] In the case $f=0$ the agreement is very satisfactory: $b=1.3$ in both cases. On the other hand, at $f=\frac{1}{2}$, $b_{\xi^+}=1.8$, and $b_\Gamma=1.1$. This discrepancy is not fully understood. From our experiments, we deduce that in the fully frustrated case the screening at T_c is somewhat larger than at $f=0$. Similar observations were also reported by van Wees, van der Zant, and Mooij[27] in a 128×384 tunnel junction array using a different experimental approach.

In conclusion, our experiments provide evidence for a vortex unbinding transition in fully frustrated Josephson junction arrays both below and above T_c: below T_c the helicity modulus and above T_c the free vortex correlation length follow the theoretical KTB predictions. The results are also consistent with Monte Carlo calculations on the fully frustrated XY model. What the experiments do not tell us is whether or not the presence of domain walls modifies the vortex-antivortex binding energy, therefore lowering the critical temperature, or if the transition is triggered by the breaking of $\frac{1}{4}$ vortex pairs, sitting at the corners of domain walls, as postulated by Halsey.[10]

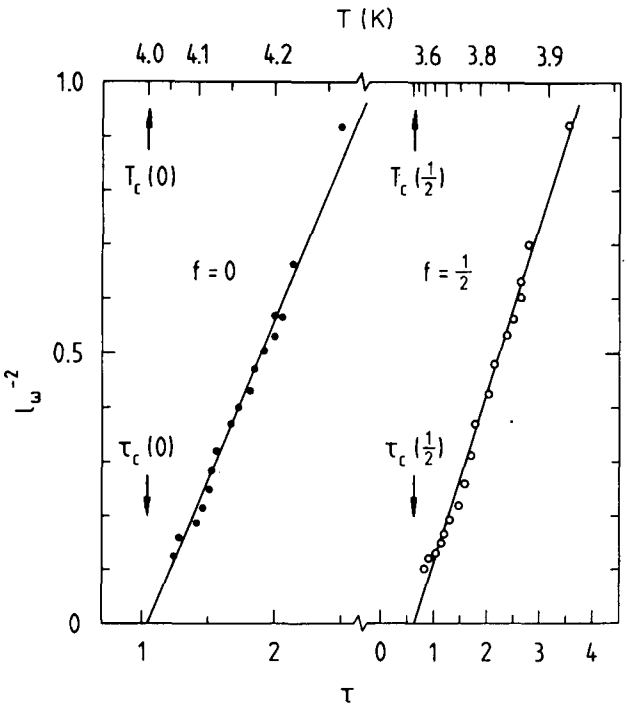

FIG. 3. Scale parameter l_ω^{-2} as a function of the reduced temperature τ for $f=0$ and $f=\frac{1}{2}$.

It is a pleasure to express our gratitude to C. Nussbaum for his expert assistance with the computer calculations. This work was supported by the Swiss National Science Foundation.

[1] J. Villain, J. Phys. (Paris) **36**, 581 (1975).
[2] M. Tinkham, D. W. Abraham, and C. J. Lobb, Phys. Rev. B **28**, 6578 (1983).
[3] S. Teitel and C. Jayaprakash, Phys. Rev. Lett. **51**, 1999 (1983); Phys. Rev. B **27**, 598 (1983).
[4] B. Pannetier, J. Chaussy, R. Rammal, and J. C. Villegier, Phys. Rev. Lett. **53**, 1845 (1984).
[5] Ch. Leemann, Ph. Lerch, G. A. Racine, and P. Martinoli, Phys. Rev. Lett. **56**, 1291 (1986).
[6] H. I. Bhushan, R. H. Cantor, J. M. Gordon, A. M. Goldman, and F. Yu, IEEE Trans. Magn. **MAG-23**, 1122 (1987).
[7] J. P. Carini, Phys. Rev. B **38**, 63 (1988).
[8] Q. Niu and F. Nori, Phys. Rev. B **39**, 2134 (1989).
[9] K. K. Mon and S. Teitel, Phys. Rev. Lett. **62**, 673 (1989).
[10] T. C. Halsey, Phys. Rev. B **31**, 5728 (1985); J. Phys. C **18**, 2437 (1985); Phys. Rev. Lett. **55**, 1018 (1985).
[11] D. H. Lee, J. D. Joannopoulos, J. W. Negele, and D. P. Landau, Phys. Rev. B **33**, 450 (1986).
[12] Ch. Leemann, Ph. Lerch, R. Théron, and P. Martinoli, Helv. Phys. Acta **60**, 128 (1987).
[13] P. G. De Gennes, Rev. Mod. Phys. **36**, 225 (1964).
[14] B. Jeanneret, J. L. Gavilano, G.-A. Racine, Ch. Leemann, and P. Martinoli, Appl. Phys. Lett. **55**, 2336 (1989).
[15] A. F. Hebard and A. T. Fiory, Physica **B&C 109-110**, 1637 (1982).
[16] V. Ambegaokar, B. I. Halperin, D. R. Nelson, and E. D. Siggia, Phys. Rev. Lett. **40**, 783 (1978); Phys. Rev. B **21**, 1806 (1980).
[17] S. R. Shenoy, J. Phys. C **18**, 5163 (1985).
[18] P. Martinoli, Ch. Leemann, and Ph. Lerch, in *Nonlinearity in*

Condensed Matter, edited by A. Bishop, D. Campbell, P. Kumar, and S. E. Trullinger, Springer Series in Solid State Sciences Vol. 69 (Springer-Verlag, Berlin, 1987), p. 361.
[19]A. T. Fiory and A. F. Hebard, Phys. Rev. B **25**, 2073 (1982).
[20]P. Martinoli, Ph. Lerch, Ch. Leemann, and H. Beck, Jpn. J. Appl. Phys. **26**, Suppl. 26-3, 1999 (1987).
[21]C. J. Lobb, D. W. Abraham, and M. Tinkham, Phys. Rev. B **27**, 150 (1983).
[22]T. Ohta and D. Jasnow, Phys. Rev. B **20**, 139 (1979).
[23]P. Minnhagen, Phys. Rev. B **32**, 7548 (1985).
[24]J. M. Kosterlitz and D. J. Thouless, J. Phys. C **6**, 1181 (1973).
[25]B. I. Halperin and D. R. Nelson, J. Low Temp. Phys. **36**, 599 (1979).
[26]J. E. Mooij, in *Percolation, Localization and Superconductivity,* edited by A. M. Goldman and S. A. Wolf (Plenum, New York, 1984) p. 325.
[27]B. J. van Wees, H. S. J. van der Zant, and J. E. Mooij, Phys. Rev. B **35**, 7291 (1987).

Frustration effects in triangulnr Josephson junction arrays

R. Theron, J.B. Simond, J.L. Gavilano*, Ch. Leemann and P. Martinoli

Institut de Physique, Université de Neuchâtel, CH-2000 Neuchâtel
*Laboratorium für Festkörperphysik, ETH Hönggerberg, CH-8093 Zürich

Using an inductive technique, the ac conductance G of two-dimensional (2D) triangular arrays of proximity effect Josephson junctions was measured as a function of temperature and frustration f (f=applied magnetic flux per unit cell of the array in units of flux quanta). G is periodic in f with period one and exhibits numerous structures corresponding to commensurability between array and vortex lattice. At low temperatures, the strength of the structures is in satisfactory agreement with mean field predictions. A narrowing of the structures at high temperatures is attributed to 2D phase fluctuations.

Two-dimensional (2D) arrays of Josephson junctions exposed to a magnetic field are a practical realization of the frustrated XY model, a system of great theoretical interest in statistical mechanics. Among the various XY lattice structures which have been theoretically studied so far [1,5], the triangular one is expected to exhibit a particularly rich critical behaviour, including the possible existence of double transitions [1]. Josephson arrays on a triangular lattice provide therefore an attractive 2D system for experimental investigations. In this paper we present a preliminary study of the complex ac conductance of a triangular array of proximity effect Josephson junctions as a function of frustration being measured by a parameter f expressing the flux per unit cell normalized to the flux quantum. From the conductance data we extract the array's inverse kinetic inductance $1/L_K(f,T)$, a quantity which can be compared with theoretical calculations [1] of the helicity modulus $\Gamma(f,T)$ of the XY model, since $1/L_K \propto \Gamma$ [1,3].

The array consists of 10^6 Pb/Cu/Pb junctions distributed on a triangular lattice with a lattice parameter a of 15 μm. To suppress undesired diffraction-like modulation effects of the ac response due to the finite size of the individual junctions, their area was reduced to 2/100 of the unit cell area. The ac conductance of the array was measured by a two coil technique described in detail elsewhere[4]. A change in the sample's conductance induces a change in the coil's mutual inductance which is detected by an RF SQUID. The sensitivity achieved with this method is $7\text{x}10^{-5}\phi_0$ per unit cell at a driving angular frequency of 1000 Rad/s. Temperatures were stabilized to better than 1 mK.

In Fig. 1 we show typical real and imaginary parts of the mutual inductance change M, (normalized to the value, M_{ss}, corresponding to perfect screening [4]) as a function of f and at T = 2.645 K, a temperature well below the array's transition temperature for $f = 0$ ($T_c(f = 0) \approx 4K$). Only data lying between $f = -1/2$ and $f = 1/2$ are shown, the response being periodic in f (with period 1) and symmetric about $f = 1/2$. The real part roughly reflects the superfluid response of the array, whereas the imaginary part is a measure of the dissipation occuring in the system [3]. We observe a very rich structure at rational values of f (with decreasing strengh at f = 0,1/2, 1/4, 1/3, 3/8, 2/5, 1/6, 1/12) corresponding to commensurate configurations of the field induced vortex lattice with the periodic pinning potential provided by the array. The peaks and dips shown in Fig. 1 are more pronounced than those predicted by mean field calculations [1] and exhibit a remarquable cusp-like shape.

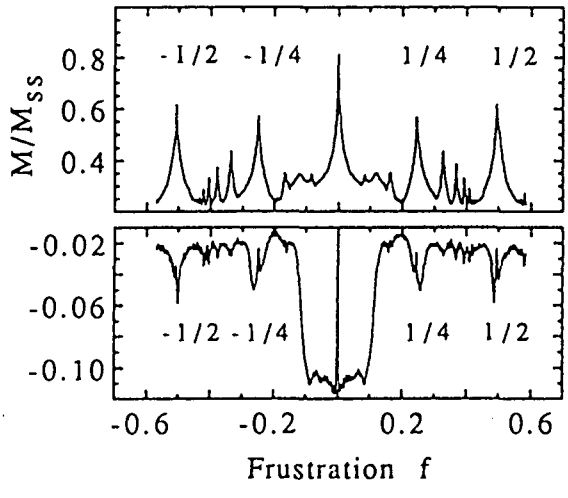

Figure 1: Real (top) and imaginary (bottom) part of the normalized change in mutual inductance M/M_{ss} as a function of f, at a constant temperature of 2.645 K.

From the mutual conductance data presented in Fig. 1 we extract $1/L_K(f,T)$ using the numerical inversion procedure described in Ref. [4]. Figure 2 shows, at three different temperatures, the ratio $L_K(0,T)/L_K(f,T)$ which we now compare with the theoretical predictions at $T = 0$ [1] in Fig. 3. We first notice that, at low temperatures, the commensurate structures emerge from a background that, regardless of the value of f, never vanishes. A plausible interpretation of this behaviour is that, at the characteristic time scale of our experiments ($\tau \approx \omega^{-1} \approx 10^{-3}s$, an irrationnaly frustrated array of finite size is in a metastable superconducting state, in contrast with the non-superconducting ($T_c(f) = 0$ for f irrational) equilibrium ($\tau \to \infty$) behaviour expected for an infinite system [5]. As for the low temperature commensurate structures, we observe that peaks at $f = 1/2$ and $1/4$ have roughly the same height, as predicted by theory (see Fig. 3) their amplitude, however, is somewhat less than the expected one (0.5). The peak at $f = 1/3$ is 0.2 high instead of $4/9 = 0.44$, the deviations from the $T = 0$ theoretical prediction of Fig. 3 becoming even more pronounced for higher order ($n > 4$) structures.

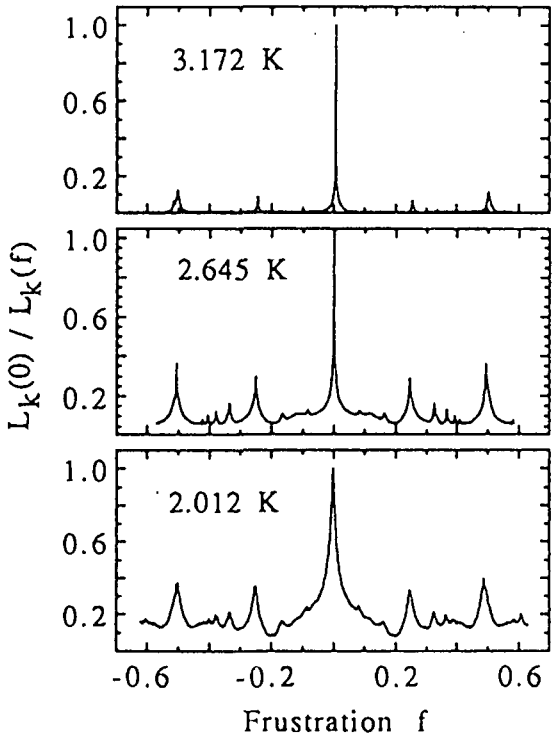

Figure 2: Normalized inverse kinetic inductance $L_k(0)/L_k(f)$ as a function of f for different temperatures.

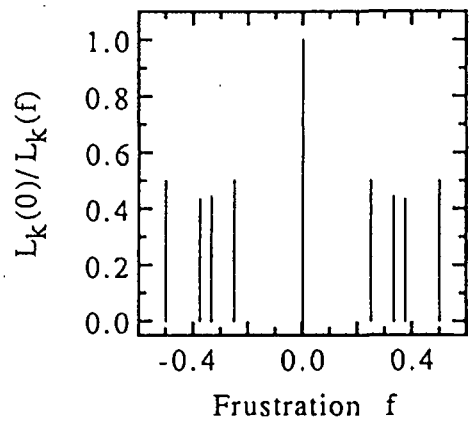

Figure 3: Theoretical prediction for $L_k(0)/L_k(f)$ as a function of f at zero temperature from Ref. 2.

This can be explained if one recognizes that higher-order commensurate vortex state have a relatively low $T_c(f)$, so that, even at the lowest temperature of Fig. 2, these vortex configuration are close to the fluctuations dominated regime near $T_c(f)$, where the results of Fig. 3 no longer apply. The importance of 2D fluctuations can be also observed by following the temperature evolution of a given peak in Fig. 2. As T increases, the amplitude of the peaks decreases and their width narrows quite dramatically into a delta-like function. Similar observations have been made in numerical simulations [6]. We attribute this behaviour to the presence of thermally activated free vortices which results in a drastic suppression of (quasi) long-range phase coherence for slightly off-match vortex configurations.

This work was supported by the Swiss National Science Foundation.

[1] W. Y. Shih and D. Stroud, Phys. Rev. B 32, 158 (1985).

[2] M.Y. Choi and S. Doniach, Phys. Rev. B 31, 4516 (1985).

[3] P. Martinoli, Ph. Lerch, Ch. Leemann, and H. Beck, Jpn J. Appl. Phys. 26, suppl. 26-3, 1999 (1987).

[4] B. Jeanneret, J.L. Gavilano, G.A. Racine, Ch. Leemann, and P. Martinoli, Appl. Phys. Lett. 55, 2336 (1989).

[5] M.Y. Choi and D. Stroud, Phys. Rev. B 35, 7109 (1987).

[6] Qian Niu and Franco Nori, Phys. Rev. B 39, 2134 (1989).

Liste des publications† et des travaux non publiés

Juin 1994

1) " Quelques aspects dynamiques des transitions de phase de Kosterlitz-Thouless dans les réseaux de jonctions Josephson." Travail de diplôme, Université de Neuchâtel, 1986.

2†) " The Kosterlitz and Thouless phase transition in Josephson junction arrays ", Ch. Leemann, Ph. Lerch, R. Théron, and P. Martinoli, Helv. Phys. Acta 60, 128 (1987).

3†) " Dynamic conductance of a 2D array of Josephson junctions ", Ph. Lerch, R. Théron, Ch. Leemann and P. Martinoli, IEEE Trans. Mag-23, 1126 (1987).

4) " Transitions de phase de réseaux de jonctions Josephson sous champ magnétique ". Réunion d'automne 1988 de la Société Suisse de Physique, présentation orale.

5†) " Dynamics of the phase transition in proximity effect arrays of Josephson junctions at full frustration ", Ph. Lerch, Ch. Leemann, R. Théron, and P. Martinoli, Phys. Rev. B 41, 11579 (1990).

6) " Dynamical response of two-dimensional arrays of Josephson junctions in a transverse magnetic field ". Réunion de printemps 1990 de la Société Suisse de Physique, présentation orale.

7†) " Frustration effects in triangular Josephson junction arrays ", R. Théron, J.B. Simond, J.L. Gavilano, Ch. Leemann and P. Martinoli, Physica B 165 &166, 1641 (1990)

8†) " Vortex dynamics in superconducting fractal networks", R. Meyer, J.L. Gavilano, B. Jeanneret, R. Théron, Ch. Leemann, H. Beck and P. Martinoli, Phys. Rev. Lett. 67, 3022 (1991).

9) " Réseaux de jonctions Josephson: effets de frustration et dynamique des vortex." Thèse de doctorat, Université de Neuchâtel, 1992.

10†) " Superconducting vortices in triangular and square Josephson junction arrays ", P. Martinoli, R. Théron, J.-B. Simond, R. Meyer, Y. Jaccard and Ch. Leemann, Physica Scripta T49, 176 (1993).

11†) " Evidence for nonconventional vortex dynamics in an ideal two-dimensional superconductor ", R. Théron, J.-B. Simond, Ch. Leemann, H. Beck, P. Minnhagen and P. Martinoli, Phys. Rev. Lett. 71, 1246 (1993).

12†) " Domain-wall superlattice states in a triangular Josephson junction array", R. Théron, S. E. Korshunov, J.-B. Simond, Ch. Leemann and P. Martinoli, Phys. Rev. Lett. 72, 562 (1993).